European Journal of Pharmaceutics and Biopharmaceutics 165 (2021) 337–344

Contents lists available at ScienceDirect

European Journal of Pharmaceutics and Biopharmaceutics

journal homepage: www.elsevier.com/locate/ejpb

Screening of metabolites in the treatment of liver cancer xenografts HepG2/ADR by psoralen-loaded lipid nanoparticles

Lihong Li [a,1], Tengteng Zou [a,1], Min Liang [b,1], Yaroslav Mezhuev [c], Aristidis Michael Tsatsakis [d], Aleksandra Buha Đorđević [e], Meng Lan [a], Fengjie Liu [a], Tiange Cai [f,*], Peng Gong [g,*], Yu Cai [a,h,i,*]

[a] College of Pharmacy, Jinan University, Guangzhou, Guangdong 510632, PR China
[b] Guangzhou Hospital of Integrated Traditional Chinese and Western Medicine, Guangzhou 510800, PR China
[c] Mendeleev University of Chemical Technology of Russia, Miusskaya sq 9, 125047 Moscow, Russia
[d] Laboratory of Toxicology, Medical School, University of Crete, Voutes, Heraklion Crete 71003, Greece
[e] Department of Toxicology "Akademik Danilo Soldatović", University of Belgrade, Faculty of Pharmacy, Vojvode Stepe 450, Belgrade, Serbia
[f] College of Life Sciences, Liaoning University, Shenyang 110036, PR China
[g] Department of General Surgery, Shenzhen University General Hospital & Carson International Cancer Research Centre, Xueyuan Road 1098, 518055 Shenzhen, PR China
[h] Cancer Institute of Jinan University, Guangzhou, Guangdong 510632, PR China
[i] Guangdong Key Lab of Traditional Chinese Medicine Information Technology, Jinan University, Guangzhou 510632, PR China

ARTICLE INFO

Keywords:
Metabolomics
Biomarkers
Nanoparticles
Liver cancer
Psolaren
Encapsulation

ABSTRACT

Objective: Our study aimed to find potential biomarkers for drug resistance in liver cancer cells using metabolomics and further to evaluate the potential of psoralen-loaded polymer lipid nanoparticles (PSO-PLNs) to reverse the resistance of cells to doxorubicin.

Methods: We used LC-MS-based non-targeted metabolomics, also known as global metabolite profiling, to screen in serum and urine of mice engrafted with a liver cancer cell line sensitive (HepG2/S) or resistant to doxorubicin (HepG2/ADR) for differentially regulated metabolites. We subsequently quantified the abundance of these metabolites in serum and the urine of mice. The mice were engrafted with HepG2 cells resistant against doxorubicin and were treated with I) doxorubicin, II) a combination of doxorubicin and psoralen and III) a combination of doxorubicin and psoralen packed in polymer lipid nanoparticles.

Results: Metabolites found to be differentially present in urine of mice engrafted with resistant HepG2 cells were: hippuric acid, hyaluronic acid, pantothenic acid, and betaine; retinoic acid and α-linolenic acid were found to be reduced in serum samples of mice with HepG2 cells resistant to doxorubicin. The targeted analysis showed that the degree of regression of metabolic markers in groups differed: treatment group 2 had stronger degree of regression than treatment group 1 and the negative control group had the smallest, which indicates that the PSO-PLNs have superior properties compared with other treatments.

Conclusion: Psoralen reverses drug resistance of liver cancer cells and its efficacy can be increased by encapsulation in polymer lipid nanoparticles.

1. Introduction

Metabolomics can be defined as the "real-time monitoring of changes in the body's function in response to for instance exogenous disturbances by following changes in metabolite abundance" [1]. Indeed, biological systems will respond to any stimulus with changes in the abundance of small endogenous molecules in vivo. Liquid Chromatography coupled to Mass Spectrometry (LC-MS) is currently the most popular technic for metabolomics due to its sensitivity and the broad range of metabolites which can detect. LC-MS-based metabolomics comes in two flavors, targeted and non-targeted metabolomics. The latter is also known as global metabolite profiling. Non-targeted metabolomics aims to analyze metabolite abundance in an unbiased manner. By comparing different experimental groups, non-targeted

* Corresponding authors at: College of Pharmacy, Jinan University, Guangzhou, Guangdong 510632, PR China (Y. Cai).
E-mail addresses: caitiange@163.com (T. Cai), doctorgongpeng@szu.edu.cn (P. Gong), caiyu8@sohu.com (Y. Cai).
[1] The authors contribute equally to the work.

https://doi.org/10.1016/j.ejpb.2021.05.025
Received 8 February 2021; Received in revised form 20 May 2021; Accepted 25 May 2021
Available online 29 May 2021

metabolomics is an excellent attractive way to screen for unanticipated metabolites that are differentially present. Found differences can subsequently be studied in more detail using more targeted approaches.

Metabolomics-based approach has been extensively used and explored as a way to find biomarkers for early diagnosis of diseases, toxicology, pharmacology, drug development and nutrition science [2–8]. Using metabolomics, it was found that levels of glycocholic acid, N-palmitoyl glutamic acid, and acety-l-carnitine in the blood allowed discriminating between pancreatic cancer and pancreatitis. Although further research is needed, quntifying these metabolites in plasma may eventually be used in the diagnosis of pancreatic ductal adenocarcinoma [9]. Using NMR-based metabolomics techniques to study the toxicity of lambda-cyhalothrin (LCT) to goldfish, the results showed that LCT had tissue-specific damage to the brain, heart, liver and kidney of goldfish. LCT not only affected the levels of many metabolites, but also breaked the balance of neurotransmitters, induces oxidative stress, and disrupts energy and amino acid metabolism. The significance of the glutamate-glutamine-γ-aminobutyric acid axis in LCT-induced toxicity was first confirmed [10]. Similarly, using metabolomics to predict liver toxicity and mode of action in vitro in HepG2 cells, the procedure revealed concentration–response effects and patterns of metabolome changes that are consistent with different liver toxicity mechanisms (liver enzyme induction/inhibition, liver toxicity, and peroxisome proliferation). Their findings provide evidence that identifying organ toxicity can be achieved in a robust, reliable, human-relevant system, representing a non-animal alternative for systemic toxicology [11]. The results suggest that metabolomics methods can be used to elucidate potential drug toxicological effects and underlying mechanisms.

It was proposed that the “Drug Metabolomics” approach can be used to achieve individualized dosing regimens. After giving paracetamol to rats, it was found that the results of the histological examination were statistically correlated with the biochemical metabolic profile of urine before administration. That is, “Drug Metabolomics” can be used as a basis for population screening. According to the special circumstances of the individual, predict the effect of the drug, change the dosage or select a certain type of drug for treatment [12]. However, there are few studies currently used to evaluate the reversal of tumor resistance.

Nanoparticles are widely used in drug delivery. In addition to many toxicological approaches, metabolomics has also been applied to evaluate the toxicity and in vivo activity of nanomedicines. Metabolomics studies have revealed the nanotoxicity of metal oxide nanoparticles such as ZnO, SiO_2, TiO_2, and CeO_2 on lung epithelial cells in vivo and in vitro and the underlying metabolic mechanisms [13]; changes in the serum metabolome by zinc NPs in vivo may be associated with inhibition of breast cancer growth and progression [14]; after synergistic radio- and photodynamic therapy with CeF_3 NPs codoping Tb^{3+} and Gd^{3+} (CeF_3: Gd^{3+}, Tb^{3+}), differential serum metabolites during tumor progression and regression may serve as reliable biomarkers for early evaluation of disease status and prognosis [15]. However, compared to metal based NPs, organic NPs lack metabolomic efforts in terms of their in vivo cytotoxicity and activity.

Psoralen (PSO), known as furanocoumarins representing chemical compounds with different potentials, is extracted from the fruits of the leguminous psoralen. They are present in edible plants as a plant secondary metabolites (phytoalexins), and considered natural toxins acting as protectors against fungi, insects, and herbivores [16]. Studies have shown that psoralen has the function of reversing the multidrug resistance of tumors [17,18]. However, it is almost insoluble in water and has poor stability (light breaks it down easily), which limits its use. Our previous studies invented psoralen-loaded lipid nanoparticles (PSO-PLNs) with lipid shell and PLGA core for sustained and controlled release of PSO. At the same time, it was found to enhance the efficacy of Doxorubicin (DOX) by reversing the resistance of tumor cells [19]. In the present study, using a combination of untargeted and targeted metabolomics, we discovered and identified a set of biomarkers of doxorubicin resistance and utilized these markers to evaluate the effect of PSO-PLNs in reversing doxorubicin resistance in liver cancer, which may be helpful to further understand the mechanism of action of PSO on drug resistence.

2. Materials and methods

All experiments were performed with mycoplasma-free cells.

2.1. Materials

PSO (greater than98% purity) was purchased from Chengdu Pufeide Biotechnology Co., Ltd. (Sichuan, Chengdu, China). Doxorubicin hydrochloride (DOX) was obtained from Selleck Chemicals (Houston, TX, USA). Cell Counting Kit-8 (CCK-8) was obtained from Dojindo Molecular Technologies, Inc. (Kumamoto, Japan). RPMI-1640 cell culture medium, penicillin–streptomycin and trypsin-EDTA were purchased from Thermo Fisher Scientifc, Inc. (Waltham, MA, USA). Fetal bovine serum (FBS) was provided by AusGenex Pty, Ltd. (Molendinar, Queensland, Australia). Sodium azide was supplied by Shandong Sino Chemical Co., Ltd. (Shandong, Jinan, China). Pentobarbital sodium was from Guangzhou Chemical Pharmaceutical Factory (Guangdong, Guangzhou, China). The PSO-PLNs (mean diameter: 80 nm, ζ potential: −25 mV, encapsulation efficiency 66%, drug loading 2.4%, Transmission electron microscopy (TEM) was used to monitor Characteristics of the PSO-PLNs) were produced by the Department of Traditional Chinese Medicine of Jinan University (Guangdong, Guangzhou, China) using an emulsifcation-solvent-evaporation (ESE) technology. The method for production of PSO-PLNs, their size, shape, and release patterns for the included doxorubicin have been described previously [19]. Water, methanol, acetonitrile and formic acid were purchased from CNW Technologies GmbH (Düsseldorf, Germany). L-2-chlorophenylalanine was from Shanghai Hengchuang Bio-technology Co., Ltd. (Shanghai, China). All chemicals and solvents were analytical or HPLC grade.

2.2. Preparation of PSO-PLNs

The method for production of PSO-PLNs with a lipid shell and a PLGA core for sustained and controlled release of PSO have been described previously [19]. Simply, using emulsification-solvent-evaporation (ESE) method, phosphatidylcholine (PC) and pegylated phospholipids (DSPE-PEG2000) were dissolved in ethanol to form the aqueous phase, which was heated at 37 °C for dispersion. PLGA or PLGA/PSO was dissolved in acetonitrile to form the oil phase, which was then added to the preheated aqueous phase. The solution was subsequently stirred for 90 min to allow for the lipids to self-assemble and the organic solvent to evaporate. The PSO-PLNs (mean diameter: 80 nm, ζ potential: −25 mV, encapsulation efficiency 66%, drug loading 2.4%) were produced by the Department of Traditional Chinese Medicine of Jinan University (Guangdong, Guangzhou, China).

2.3. Experimental animals and tumor cell line

Athymic nude mice (nu/nu-BALB/c), 5 weeks old, equal numbers of males and females, were provided by Beijing Huafu Kang Biotechnology Co., Ltd (Beijing, China), and were maintained in our facility with free access to water and food, under a 12-h light/dark cycle, with 40% humidity.

Tumor cell lines: hepatoblastoma HepG2 cells sensitive (HepG2/S) and resistant to DOX (HepG2/ADR) were provided by Nanjing KeyGen Biotech Co., Ltd. (Nanjing, Jiangsu, China).

2.4. Methods

2.4.1. Establishment of animal tumor cell line model

2.4.1.1. Cell culture. HepG2/S and HepG2/ADR were maintained and grown in RPMI-1640 medium supplemented with 10% (v/v) FBS and 1% (v/v) penicillin–streptomycin in a humidifed atmosphere with 5% CO_2 at 37 ℃. For the DOX-resistant HepG2 cell cultures, 1 μM DOX was added to the RPMI-1640 medium every three passages to maintain drug resistance. Cells were used for experiments once they reached 80% confluency.

2.4.1.2. Grafting of tumor cell lines. HepG2/S and HepG2/ADR cells (each 6×10^7cells/mL in PBS*0.2 mL/mouse) were subcutaneously injected into the shoulder region of 20 healthy nude mice. To increase transplant success, matrigel (Corning, 354354248, 20.70 mg/mL) was added to the collected cell liquid. Two weeks after implantation, mice with approximately the same tumor cell burden (diameter 6–8 mm) were selected for subsequent experiments. The subcurtaneous tumor mass was collected, the central necrotic area (~4 mm diameter) was removed, while after theremaining tumor mass was divided into small pieces of about 2 mm^3, which were transplanted subcutaneously into the axillary region of nude mice.

2.4.2. Non-targeted metabolomics study

2.4.2.1. Sample collection. Urine was collected in metabolic cages (Nanjing Diagnostic Biotechnology Co., Ltd.). It was preserved with 1% sodium azide solution (10 μL for about 1 mL urine). Urine samples were subsequently centrifuged at 4℃ for 10 min (3000 g). The supernatant was collected in pre-cooled low protein adsorption 1.5 mL tubes (Eppendorf, Germany) and stored at −80 °C till analysis.

Serum was prepared from blood collected by cardiac puncture from mice deeply anesthetized with sodium pentobarbital (1%, 0.1–0.15 mL/each mouse). After leaving the blood at room temperature for 30 min, serum was prepared by centrifugation (700*g*/4900*g*, 4 °C, 10 min) and stored in a low protein adsorption tubes (Eppendorf, Germany) at −80 °C.

2.4.2.2. Sample preparation for LC-MS analysis. 150 μL of urine or serum was centrifuged at 12,900*g* for 10 min at 4℃. 100 μL of the supernatant was transferred to a 1.5 mL PE tube containing 10 μL of 2-chloro-L-phenylalanine (0.3 mg/mL, dissolved in methanol used as internal standard). After vortexing the tube for 10 s, 100 μL or 300 μL of an ice cold mixture of methanol and acetonitrile (2/1, v/v) was added to urine and serum samples, respectively. The mixtures were then vortexed for 1 min, ultrasonicated in an ice water bath for 10 min and stored at −20℃ for 30 min. After centrifugation at 12,900*g* at 4℃ for 15 min, the organic phase of supernatants were evaporated by Nitrogen blower (Hanon Instrument Co., Ltd., Shanghai, China) and stored at 4 °C prior to analysis. The samples were dissolved in HPLC grade water (1:1 ratio of original sample volume to water), vortex mixed and centrifuged at 12,900*g* for 15 min. The supernatants were transferred to LC vials and analyzed.

Quality control (QC) samples were prepared by mixing aliquots of equal volumes of all samples.

2.4.2.3. LC/MS analysis. LC (ACQUITY UPLC I-Class, Waters, USA) was done on an Acquity BEH C18 column (100 mm × 2.1 mm i.d., 1.7 μm; Waters, Milford, USA). The column was maintained at 45 °C and separation was achieved using the following gradient: 1–30% B over 0–1 min, 30–60% B over 1–2.5 min, 60–90% B over 2.5–6.5 min, 90–100% B over 6.5–8.5 min, the composition was held at 100% B for 2.2 min, then 10.7–10.8 min, 100% to 1% B, and 10.8–13 min holding at 1% B at a flow rate of 0.40 mL/min, where B was the mobile phase acetonitrile/methanol 2/3 (v/v) (0.1% (v/v) formic acid) and Aaqueous formic acid (0.1% (v/v) formic acid). The injection volume was 1 μL. Mass spectrometric data was collected on a Waters VION IMS Q-TOF Mass Spectrometer equipped with an electrospray ionization (ESI) source operating in either positive or negative ion mode. The capillary voltages, DP, CE were 2.5 kV, 40 V and 6 eV, respectivey. Source temperature and desolvation temperature was set at 115℃ and 450℃, respectively, with a desolvation gas flow of 900 L/h. Centroid data was collected from 50 to 1,000 *m/z* with a scan time of 0.2 s and interscan delay of 0.02 s over a 13 min analysis time. The QCs were injected at regular intervals (every 8 samples) throughout the analytical run to assess repeatability.

2.4.2.4. Data processing. Prior to pattern recognition, LC/MS raw data were subjected to baseline filtration, peak identification, integration, retention time correction, peak alignment, and normalization using the metabolomics processing software package progenesis QI (Waters Corporation, Milford, USA). This yielded a matrix with positive and negative ion data with retention time, mass-to-charge ratio and peak intensity.

2.4.2.5. Multivariate statistical analysis. The processed data matrix was subsequently imported into the SIMCA software package (version 14.0, Umetrics, Umeå, Sweden), and analyzed using unsupervised Principal Component Analysis (PCA) to observe the overall distribution between samples and the stability of the entire analysis process by the degree of aggregation of QC samples. Supervised Orthogonal Partial Least Squares Discriminant Analysis (OPLS-DA) was used to detect differentially present metabolites in the metabolic profiles between the groups and to identify potential biomarkers. To prevent over-fitting and test the quality of the model, we used seven-cycle interactive verification and 200 response permutation testing (RPT).

2.4.2.6. Screening and identifiction of metabolic markers. Multi-dimensional and single-dimensional methods were used to screen for metabolic markers that could discriminate between the two groups. Multidimensional methods used include: metabolites away from the center point in the s-plots loading map; metabolites with higher pq value on the principal component of the Loading plot histogram; metabolites with VIP value greater than 1.5 on the first principal component in the OPLS-DA model. In the volcano map analysis, when the difference multiple is 2, the metabolite with a higher value of -log 10 (P-value). Heat map to view general trends and verify selected metabolic markers. The single-dimensional method included determination of the statistical significance by multiple T-test (between 2 groups). $P < 0.01$ was considered to indicate a statistically significant difference. Potential biomrakers had to meet the above listed requirements. Determine the up-and-down information by the ratio of the average content of metabolites in the two sets of samples (fold change, FC, If the substance has a $FC > 6/5$ in two sets of samples, it is an up-regulated metabolite. Conversely, if $FC < 5/6$, it is a down-regulated metabolite). Progenesis QI (Waters Corporation, Milford, USA) Metadata Processing Software and publicly available databases such as http://www.hmdb.ca/ and http://www.lipidmaps.org/ were used to putatively identify differentially present metabolites, and then the structures of these compounds were analyzed based on the MS/MS fragments and exact mass information obtained by HPLC-Q-TOF-MS/MS. Moreover, their identification was confirmed using the corresponding standard compounds.

2.4.3. Targeted metabolomics analysis

Quantitative analysis of the selected metabolic markers (urine: hippuric acid, pantothenic acid, hyaluronic acid, and betaine; serum: retinoic acid and a-linolenic acid) was performed on a Shimadzu LC-30AD HPLC analytical system (Shimadzu Co., Kyoto, Japan) coupled to an AB SCIEX 4500 triple quadrupole Mass Spectrometer equipped with an ESI source (AB SCIEX Co., Redwood City, CA, USA). The relative abundance of the biomarkers was used to evaluate the reversal of resistance after

the administration of PSO-PLNs. Characterization of tumor cell resistance is a change in the expression of metabolites. Therefore, we can use the expression results of these metabolites to evaluate the degree of tumor cell resistance (The metabolites that were originally up-regulated showed a tendency to decrease after administration, or the metabolites that were originally down-regulated showed an increasing tendency after administration, which may indicate that the drug has a reversal of drug resistance).

2.4.3.1. Mode of administration and dosage. Thirty-two nude mice with tumor formed by proliferating HepG2/ADR cells were generated as described above and divided into four groups. The first group received saline (negative control group); the second group received DOX only (treatment group 1); the third group received a combination of DOX and PSO (treatment group 2); the fourth group received DOX and PSO-PLNs (treatment group 3). Also, eight nude mice with tumors formed by proliferating HepG2/S cells received DOX (Sensitive group, also positive control group). All drugs except saline were administered via the tail vein injection (3 mg/kg, the dose of PSO-PLNs was calculated by the loaded PSO, once every three days, 0.2 mL per dose, vehicle: The prepared PSO-PLNs is lyophilized into powder and dissolved in 0.9% physiological saline before use; DOX: 0.9% physiological saline; PSO: After dissolved in injection grade soybean oil, a small amount of surfactant is added, and finally diluted with physiological saline.) with the help of a mouse tail vein injection fixture (Shanghai Yuyan Scientific Instrument Co., Ltd., Shanghai, China). Tumor size and body weight changes were recorded every two days.

2.4.3.2. Sample collection and sample processing. The same as non-targeted metabolomics described above.

2.4.3.3. LC/MS analysis. **LC Conditions**

Urine Sample Analysis parameter:

Injection Volume: 5 μL

Column Temperature: 45.0℃

Solvent: separation was achieved using the gradient in Table 1.

Column: Agilent ZORBAX Bonus-RP (150 mm × 2.1 mm 5 μm; PN: 883725–901; SN: USECO01728; USA).

Serum Sample Analysis parameter:

Injection Volume: 5 μL

Column Temperature: 45.0℃

Column: Agilent ZORBAX XDB- C18 (50 mm × 2.1 mm 3.5 μm; PN: 971700–902; SN: USHPO02791; USA).

Solvent: separation was achieved using the gradient in Table 2.

MS Conditions

The mass spectrometric data was collected using an AB SCIEX 4500 Mass Spectrometer equipped with anelectrospray ionization (ESI) source operating in either positive or negative ion mode. Metabolites were detected in Multiple Reaction Monitoring mode (MRM) and specific settings for individual metabolites are summarized in Table 3.

2.4.3.4. Data analysis. Use the corresponding metabolite standard, external standard method to quantify metabolic markers, calculate the callback rate. Callback rate was then calculated using the following formula:

$$\text{Callback rate}\% = (C - A)/C \times 100\%$$

C: Concentration difference of the metabolite between the negative control group and the sensitive group.

A: Concentration difference of the metabolite between the treatment group and the sensitive group.

2.4.3.5. Statement. We confirm that all methods were performed in accordance with the relevant guidelines and regulations.

Table 1
Urine Sample Analysis parameter for LC.

Step	Total Time (min)	Flow Rate (μl/min)	B (%) water (0.2% HCOOH)	C (%) methanol
0	0	250	2	98
1	1.5	250	2	98
2	2.5	250	100	0
3	8.5	250	100	0
4	8.6	250	2	98
5	18	250	2	98

Table 2
Serum Sample Analysis parameter for LC.

Step	Total Time (min)	Flow Rate (μl/min)	A (%) water	C (%) water (0.2%HCOOH)	D (%) acetonitrile
0	0.00	500	2	5	93
1	1.00	500	100	0	0
2	5.00	500	100	0	0
3	5.10	500	2	5	93
4	10.00	500	2	5	93

3. Results

The base peak chromatogram of the quality control sample was visually monitored. It was found that the peak capacity was large, and the retention time was reproducible, indicating that the instrument analysis system was stable. Successfully generated a mouse model mimicking liver cancer, and the tumor mass was uniform among mice, however, as shown in Fig. 1, the size of the tumor was different between each group after administration in targeted metabolomics studies.

3.1. Multivariate statistical analysis

As shown in Figs. 2 and 3, the model results show that the metabolites in the two animal models are significantly different and can be classified better. At the same time, the model interpretation rate [Urine: R2X (cum) = 90.7%; Serum: R2X (cum) = 97.1%] and prediction rate [Urine: Q2 (cum) = 58.4%; Serum:Q2 (cum) = 93.5%] indicate that the model can explain and predict well the difference between the two sets of samples. The results of the response permutation testing (Urine: Q2 = -0.617 < 0; Serum: Q2 = -0.54 < 0) showed that the model did not overfitting, and they were reliable.

3.2. Determination of metabolic markers

After the combination of multidimensional and single-dimensional screening, a total of more than 50 eligible potential metabolic markers were screened. Subsequently, they were verified employing the corresponding standard compounds. Finally, the following six metabolites were found to have good reproducibility and parallelism in each biological sample, and their VIP and P-Values showed that they had significant differences between the two biological samples. Related information finally determined is shown in Table 4.

3.3. Evaluation of reversal of multidrug resistance

Metabolites in biological samples were quantified by metabolic marker standards to explore changes in the content of each metabolite under different modes of administration. As shown in Table 5, the difference in expression of these six metabolites between the sensitive group and negative control groups consistent with the results in non-targeted metabolomics, which again validates the six metabolites as metabolic markers for HepG2/ADR resistance. The results of the negative control group and the treatment group 1 (DOX) were similar,

Table 3
MRM analysis parameters of metabolic markers.

Sample	Marker	Instrument parameters	Q1	Q3	DP	EP	CE	CXP
Urine	Xanthurenic acid	CUR:30.00 CAD:High IS:5500.00 TEM:500.00 GS1:50.00 GS2:60.00	206.100	160.00	40	8	23	11
	Pantothenic acid		220.100	184.00	40	8	16	13
	Hippuric acid		180.100	104.900	46	11	18	7
	Betaine		118.000	58.000	40	7	38	10
Serum	Retinoic acid	CUR:30.00 CAD:High IS:-4500.00 TEM:500.00 GS1:50.00 GS2:60.00	299.100	255.100	−84	−14	−23	−10
	Alpha-Linolenic acid		277.100	127.00	−90	−14	−30	−9

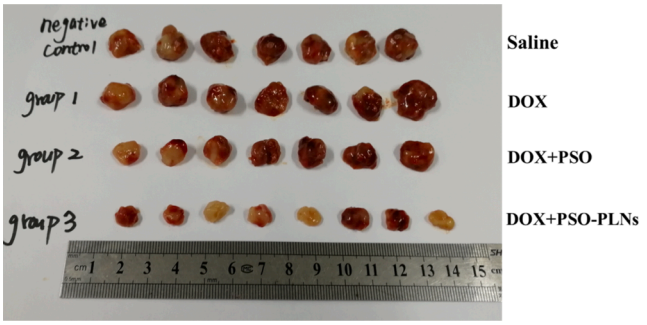

Fig. 1. Tumor size of each group in targeted metabolomics. (Tumor size: negative control group≈treatment group 1 > treatment group 2 > treatment group 3).

indicating that the chemotherapeutic drug DOX had almost no effect on the tumor cells because of the drug resistance of the cells. The callback rate of the six metabolites in the three treatment groups showed: treatment group 3 (DOX + PSO-PLNs) > treatment group 2 (DOX + PSO) > treatment group 1 (DOX), indicating that PSO has the effect of reversing the drug resistance of HepG2/ADR cells, moreover, it is better to prepare it into polymer lipid nanoparticles.

4. Discussion

Our new findings demonstrate that metabolomics approach can be used to detect drug resistance, as a more advanced approach than following tumor growth by measuring tumor dimensions. Furthermore, metabolomics is superior to other omics in many ways. It not only reflects the phenotypic changes most directly, but more importantly, also provides increased detection limits for the small changes in genes by amplifying transcription, translation, and synthesis of the protein. A disadvantage of metabolomics is that current techniques do not cover

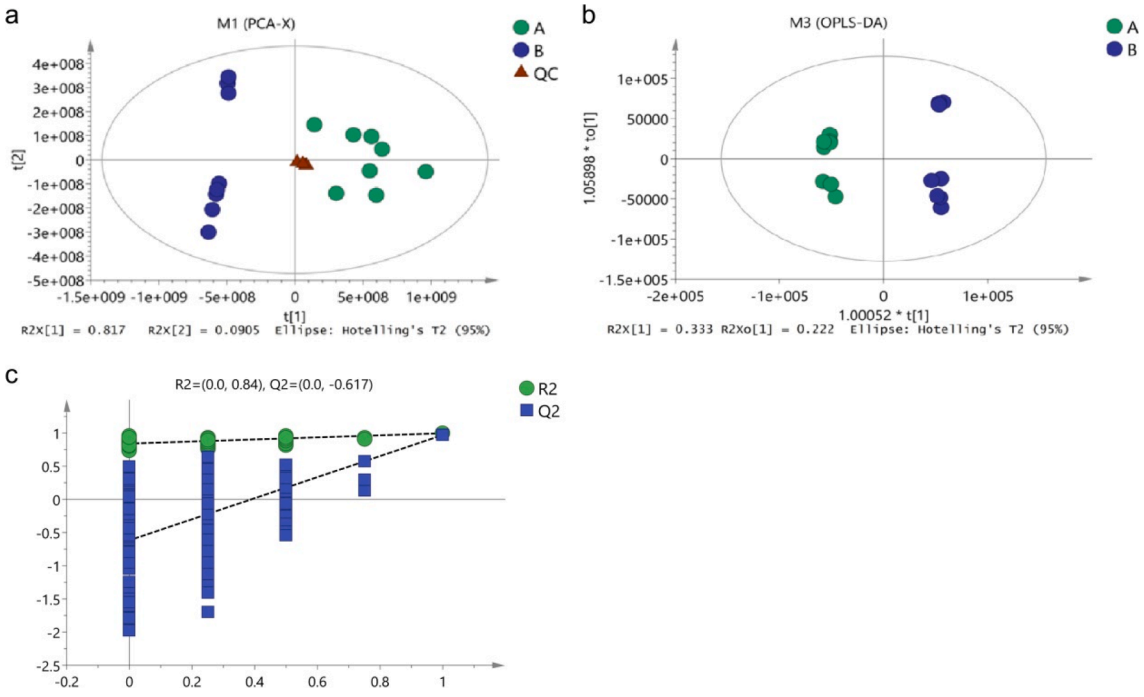

Fig. 2. Multivariate statistical scores plot and response permutation testing of urine samples. (A: Sensitive group sample; B: Drug resistant group sample; QC: Quality control sample) [a: unsupervised Principal Component Analysis (PCA), R2X (cum) = 90.7%, Q2 (cum) = 58.4%; b: Supervised Orthogonal Partial Least Squares Discriminant Analysis (OPLS-DA); c: response permutation testing (RPT), R2 = 0.84, Q2 = -0.617 < 0]

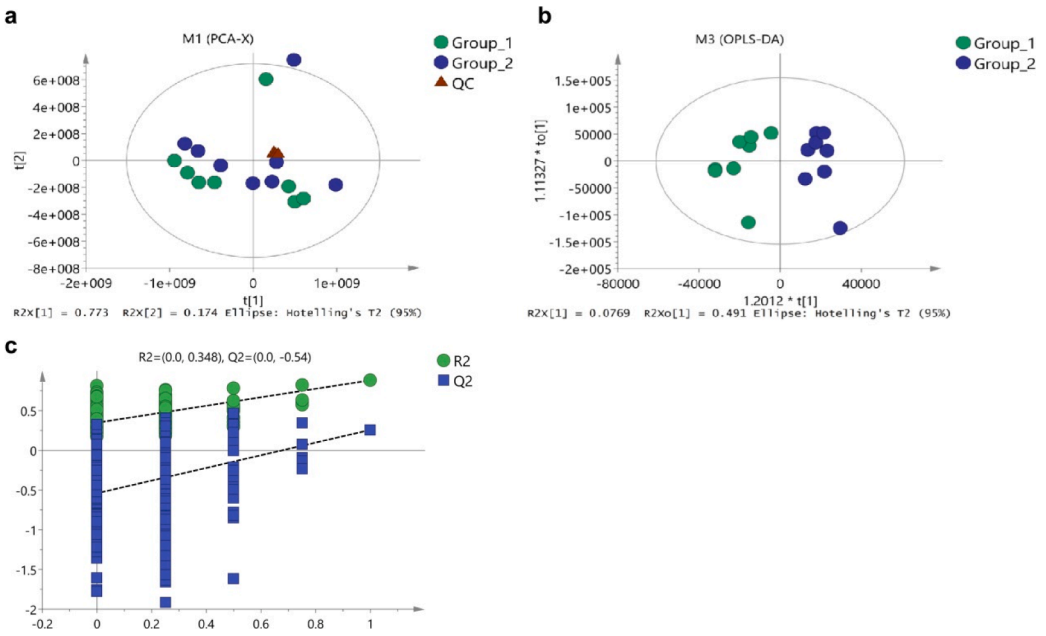

Fig. 3. Multivariate statistical scores plot and response permutation testing of serumsamples. (A: Sensitive group sample; B: Drug resistant group sample; QC: Quality control sample). [a: unsupervised Principal Component Analysis (PCA), R2X (cum) = 97.1%, Q2 (cum) = 93.5%; b: Supervised Orthogonal Partial Least Squares Discriminant Analysis (OPLS-DA); c: response permutation testing (RPT), R2 = 0.348, Q2 = -0.54 < 0]

Table 4
Summary of selected biomarker information.

sample	*m/z*	Ion mode	Metabolites	Formula	VIP	P-value	FC(B/A)	
Urine	206.0454454	POS	Xanthurenic acid	$C_{10}H_7NO_4$	21.9827	0.0111	2.74483	up
	220.1185993	POS	Pantothenic acid	$C_9H_{17}NO_5$	10.6858	0.01083	1.791477	up
	178.050613	NEG	Hippuric acid	$C_9H_9NO_3$	10.2889	8.8E-05	0.383898	down
	100.0767485	POS	Betaine	$C_5H_{11}NO_2$	9.47043	4.1E-11	16.43208	up
Serum	301.2166013	POS	Retinoic acid	$C_{20}H_{28}O_2$	2.89977	0.04012	0.534041	down
	279.2319907	POS	Alpha-Linolenic acid	$C_{18}H_{30}O_2$	2.88175	0.0359	0.375332	down

Table 5
Metabolite concentration and Callback rate of each treatment group.

Metabolites	Concentration (μg/L)					Callback ratio (%)		
	Sensitive group	negative control group	treatment group 1	treatment group 2	treatment group 3	DOX	DOX + PSO	DOX+(PSO-PLNs)
Xanthurenic acid	11.77	92.7	93.12	82.62	10.76	−0.52	12.45	101.25
Pantothenic acid	15.32	74.19	73.30	53.16	16.43	1.52	35.72	98.11
Hippuric acid	66.53	15.48	13.33	25.42	39.73	−4.21	19.48	47.50
Betaine	44.58	96.5	96.22	75.41	55.23	0.53	40.62	79.49
Retinoic acid	102.67	22.72	23.18	43.67	89.59	0.58	26.21	83.64
α-Linolenic acid	31.24	12.20	12.56	21.45	33.11	1.87	48.59	109.82

the separation and detection of all metabolites of varying molecular sizes and properties. To improve the accuracy of the experiment, other detection platforms such as GC–MS can be combined to obtain a wider range of metabolite types and a wider concentration range. In addition to the integration of analytical techniques and the integration of different tissues of organisms, metabolomics can also be combined with other omics, such as proteomics, transcriptomics, and genomics [20–23]. Hence, a multi-layered omics integration method used to study the multidrug resistance of tumor cells will achieve better chemotherapy effects and serve cancer patients.

In the non-targeted metabolomics experiment, it was found in the PCA analysis of urine samples that group B (liver cancer resistant group) showed a clear separation trend, indicating that there is a difference in the sample metabolic profile of the resistant group. There are many reasons for this phenomenon, such as sample collection, storage, transportation, pre-processing, analysis, etc. To maintain the authenticity of the data, we retained it. In the principal component analysis of serum samples, it is not easy to see a significant difference between two groups, and a biological sample of the drug resistance group is outside the 95% confidence interval. The analysis of D modx (abnormal point diagnosis) revealed abnormal points in urine and serum samples, especially serum, which means that in the process of pre-treatment and extraction, the biological sample to be detected may lose some initial metabolite information for various reasons. Namely, during the experiment, it was found that if the ambient temperature is lower than 20 °C, the urine sample collection of the animal is difficult, while excessive collection time leads to secondary degradation of metabolites, affecting the results of the experiment. Therefore, it should be noted that the ambient temperature should be raised appropriately, and the urine collection bottle should be placed on ice [24]. Furthermore, if alcohol is used to sterilize the skin when taking a blood sample, it should completely evaporate prior to sampling [25]. There are many non-

inactivated proteases in blood samples and urine samples, and there may be microbial contamination, which has a great influence on the metabolic spectrum in the sample. When these samples are placed at room temperature for more than 2 h, the cells degrade to produce a large number of metabolites. On the other hand, under the action of proteases, large proteins will degrade to produce many small peptides, which will also affect the detection of metabolic spectra. To avoid this, it is necessary to separate and freeze at −80 °C as soon as possible.

While there is no conclusive knowledge about the mechanism of the cytostatic action of doxorubicin, certain reports indicate that it is related to the proteolytic cleavage of the CREB3L1 gene encoding the synthesis of the protein, the functions of which are related to active transport through membranes [26]. Previously it was shown that in cells resistant to anthracycline derivatives including doxorubicin, an active efflux thereof is observed [27]. It is also known that curcumin [28] and genistein [29] in combination with doxorubicin increased the intracellular accumulation of doxorubicin in drug-resistant cancer cells. Doxorubicin, genistein, curcumin and psoralen used in the present paper are structurally similar through the presence of carbonyl-, ether- or hydroxyl-functionalized hydrophobic molecular fragments (Fig. 4). It appears that the functional groups of these molecules are responsible for binding to the cell membrane receptors.

Therefore, we assume that the suppression of the resistance of the HepG2/ADR cells to doxorubicin in the presence of psoralen may be related to the competitive blocking of the membrane receptors that prevent permeation of doxorubicin by psoralen. The blocking of the receptors by psoralen is possible provided that it forms stronger bonds than doxorubicin. The suggested mechanism is in good agreement with the literature data [26–29] and the investigation results presented herein. High efficiency of psoralen-containing nanoparticles to potentiate the effect of doxorubicin on drug-resistant HepG2/ADR liver cancer cells is related not only to improved distribution of psoralen but also to the carrier particle size in the range of 80–95 nm, which promotes permeation into membranes [30]. Finally, the concentration change of metabolites in urine and serum are associated with the membrane transport or regulation of gene expression, which is also consistent with the proposed mechanism of loss of resistance of HepG2/ADR cells to doxorubicin. For example, retinoic acid is involved in the regulation of the expression of many genes [31]; betaine acts as an activator of the synthesis of the cell membrane phospholipids and is involved in DNA methylation [32]; hyaluronic acid is involved in the proliferation, migration and differentiation of cells as well as in the interaction with the receptors of cell membranes [33].

It is known that the synthesis of hippuronic acid through the binding of benzoic acid and glycine is suppressed in cases of liver damage [34]. Therefore, the decreased production of hippuronic acid is indicative of liver damage. The increased therapeutic activity of doxorubicin and psoralen included into nanoparticles is consistent with a significant increase in the content of hippuric acid in group 3. The combined use of doxorubicin and free psoralen (group 2) also leads to an increase in the level of hippuronic acid compared to group 1, but a decrease compared to group 3. Thus, the content of hippuric acid, which is a marker of the functional status of the liver, is consistent with other results presented in this work.

5. Conclusions

Metabolomics research methods can be used to evaluate the reversal effect of drugs on tumor cell resistance. This study found that the potential biomarkers of HepG2/ADR-resistant liver cancer cells are: hippuric acid, hyaluronic acid, pantothenic acid and betaine in urine; retinoid acid and α-linolenic acid in serum. At the same time, it is also verified that the Chinese medicine monomer psoralen has the effect of reversing the multidrug resistance of liver cancer. Prepared into polymer lipid nanoparticles, psoralen can overcome the shortcomings of the drug substance and enhance its role in reversing tumor resistance. It has been suggested that suppression of the resistance of HepG2/ADR cells to doxorubicin in the presence of psoralen occurs due to the competition of psoralen and doxorubicin toward the shared cell membrane receptors responsible for the active efflux of doxorubicin.

6. Funding

This study was financially supported by the National Natural Science Foundation of China (grant no. 81173215); the Science and Technology Program of Guangzhou, China (grant nos. 2014J4500005, 201704030141); the Science Program of the Department of Education of Guangdong, China (grant no. 2015KGJHZ012); the Guangzhou Key Research and Development Plan, China (grant no. 202103000091); the Guangdong Key Lab of Traditional Chinese Medicine Information

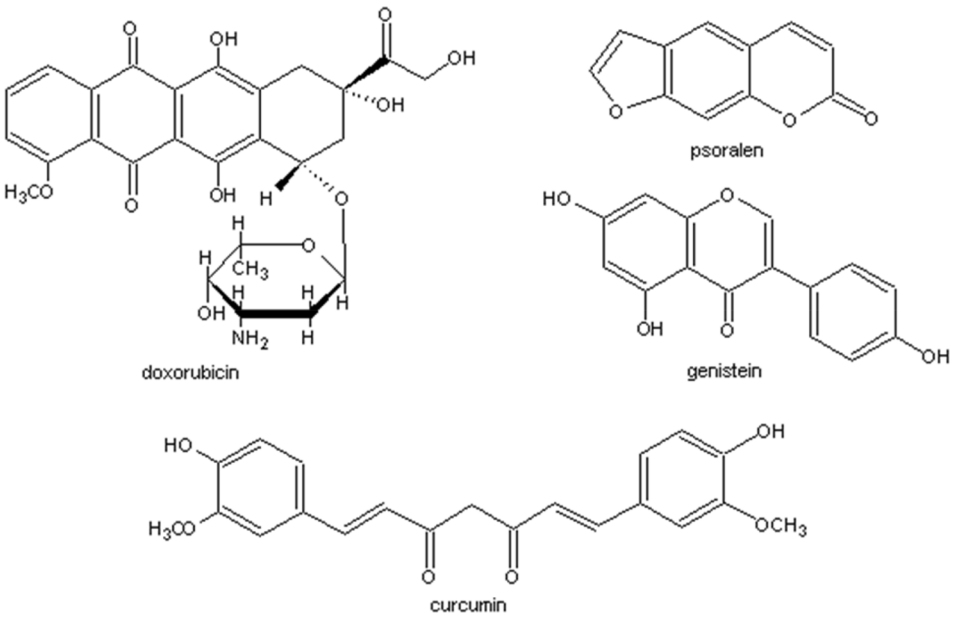

Fig. 4. Compound structure. Doxorubicin, genistein, curcumin and psoralen, which was used in the present paper are structurally similar through the presence of carbonyl-, ether- or hydroxyl-functionalized hydrophobic molecular fragments.

Technology, China (grant no. 2021B1212040007).

7. Author contributions

Lihong Li, Tengteng Zou and Min Liang performed the screening of PSO-PLNs formulation components, and were major contributors in writing the manuscript; Meng Lan was responsible for the evaluation of PSO-PLNs quality; Fengjie Liu undertook the establishment of animal models; Yaroslav Mezhuev, Aristidis Michael Tsatsakis and Aleksandra Đorđević made substantial contributionsto acquisition, analysis and interpretation of data; Tiange Cai, Peng Gong and Yu Cai were involved in drafting the manuscript and revising it critically for intellectual content, made contributions to conception and design, and assisted in the analysis of all experiments. All authors read and approved the final manuscript.

8. Ethical approval and consent to participate

The protocol for the study was approved by the College of Pharmacy, Jinan University. The Laboratory Animal Ethics Committee of Jinan University approved all protocols (date of approval, 2018.12.27; certification no. IACUC20180109-03).

9. Patient consent for publication

Not applicable.

10. Data availability statement

Data will be provided and shared after accepting this article.

Declaration of Competing Interest

The authors declare that they have no known competing financial interests or personal relationships that could have appeared to influence the work reported in this paper.

Acknowledgements

Not applicable.

Appendix A. Supplementary material

Supplementary data to this article can be found online at https://doi.org/10.1016/j.ejpb.2021.05.025.

References

[1] J.K. Nicholson, J.C. Lindon, E. Holmes, 'Metabonomics': understanding the metabolic responses of living systems to pathophysiological stimuli via multivariate statistical analysis of biological NMR spectroscopic data, Xenobiotica 29 (11) (1999) 1181–1189.
[2] L. Brennan, NMR-based metabolomics: From sample preparation to applications in nutrition research, Prog. Nucl. Magn. Reson. Spectrosc. 83 (2014) 42–49.
[3] J.B.G. Elizabeth, M.S. McNiven, C.M. Slupsky, Analytical metabolomics: nutritional opportunities for personalized health, J. Nutr. Biochem. 22 (11) (2011) 995–1002.
[4] V.M. Asiago, L.Z. Alvarado, N. Shanaiah, G.A.N. Gowda, K. Owusu-Sarfo, R. A. Ballas, D. Raftery, Early Detection of Recurrent Breast Cancer Using Metabolite Profiling, Cancer Res. 70 (21) (2010) 8309–8318.
[5] M.W. Michael J. Gibney, Lorraine Brennan, M. HelenRoche, Bruce German, Ben van Ommen, Metabolomics in human nutrition: opportunities and challenges, Am. J. Clin. Nutr. 82 (3) (2005) 497–503.
[6] M.A.R.J.B. German, L. Fay, S.M. Watkins, Metabolomics and Individual Metabolic Assessment: The Next Great Challenge for Nutrition, J. Nutrit. 132 (9) (2002) 2486–2487.
[7] X. Wang, A. Zhang, P. Wang, H. Sun, G. Wu, W. Sun, H. Lv, G. Jiao, H. Xu, Y. Yuan, L. Liu, D. Zou, Z. Wu, Y. Han, G. Yan, W. Dong, F. Wu, T. Dong, Y. Yu, S. Zhang, X. Wu, X. Tong, X. Meng, Metabolomics Coupled with Proteomics Advancing Drug Discovery toward More Agile Development of Targeted Combination Therapies, Mol. Cell. Proteomics 12 (5) (2013) 1226–1238.
[8] J.R.I. Diren Beyoglu, Metabolomics and its potential in drug development, Biochem. Pharmacol. 85 (1) (2013) 12–20.
[9] A. Lindahl, R. Heuchel, J. Forshed, J. Lehtiö, M. Löhr, A. Nordström, Discrimination of pancreatic cancer and pancreatitis by LC-MS metabolomics, Metabolomics 13 (5) (2017) 61.
[10] M. Li, J. Wang, Z. Lu, D. Wei, M. Yang, L. Kong, NMR-based metabolomics approach to study the toxicity of lambda-cyhalothrin to goldfish (Carassius auratus), Aquat. Toxicol. 146 (2014) 82–92.
[11] T. Ramirez, A. Strigun, A. Verlohner, H.-A. Huener, E. Peter, M. Herold, N. Bordag, W. Mellert, T. Walk, M. Spitzer, X. Jiang, S. Sperber, T. Hofmann, T. Hartung, H. Kamp, B. van Ravenzwaay, Prediction of liver toxicity and mode of action using metabolomics in vitro in HepG2 cells, Arch. Toxicol. 92 (2) (2018) 893–906.
[12] T. Andrew Clayton, J.C. Lindon, O. Cloarec, H. Antti, C. Charuel, G. Hanton, J.-P. Provost, J.-L. Le Net, D. Baker, R.J. Walley, J.R. Everett, J.K. Nicholson, Pharmaco-metabonomic phenotyping and personalized drug treatment, Nature 440 (7087) (2006) 1073–1077.
[13] L. Cui, X. Wang, B. Sun, T. Xia, S. Hu, Predictive Metabolomic Signatures for Safety Assessment of Metal Oxide Nanoparticles, ACS Nano 13 (11) (2019) 13065–13082.
[14] B. Bobrowska-Korczak, P. Gątarek, D. Skrajnowska, W. Bielecki, R. Wyrebiak, T. Kovalczuk, R. Wrzesień, J. Kałużna-Czaplińska, Effect of Zinc Supplementation on the Serum Metabolites Profile at the Early Stage of Breast Cancer in Rats, Nutrients 12 (11) (2020) 3457.
[15] F. Ahmad, X. Wang, Z. Jiang, X. Yu, X. Liu, R. Mao, X. Chen, W. Li, Codoping Enhanced Radioluminescence of Nanoscintillators for X-ray-Activated Synergistic Cancer Therapy and Prognosis Using Metabolomics, ACS Nano 13 (9) (2019) 10419–10433.
[16] L.C.R.C. Silva, A.Â.M. Barreto, H.H.S. Medrado, M.D. Mota, A.D.F.S. Júnior, et al., Determination of Psoralens in Child Food (Soups and Baby Food) from Brazil by High-performance Liquid Chromatography (HPLC), Food Anal. Meth. 10 (11) (2017) 3658–3665.
[17] M.-J. Hsieh, M.-K. Chen, Y.-Y. Yu, G.-T. Sheu, H.-L. Chiou, Psoralen reverses docetaxel-induced multidrug resistance in A549/D16 human lung cancer cells lines, Phytomedicine 21 (7) (2014) 970–977.
[18] J. Jiang, X. Wang, K. Cheng, W. Zhao, Y. Hua, C. Xu, Z. Yang, Psoralen reverses the P-glycoprotein-mediated multidrug resistance in human breast cancer MCF-7/ADR cells, Mol. Med. Rep. 13 (6) (2016) 4745–4750.
[19] Y. Yuan, P. Chiba, T. Cai, R. Callaghan, L. Bai, S. Cole, Y. Cai, Fabrication of psoralen-loaded lipid-polymer hybrid nanoparticles and their reversal effect on drug resistance of cancer cells, Oncol. Rep. 40 (2) (2018) 1055–1063.
[20] J.X. Joseph, E. Ippolito, Sanjay Jain, Krista Moulder, Steven Mennerick, Jan R. Crowley, R. Reid Townsend, Jeffrey I. Gordon, An integrated functional genomics and metabolomics approach for defining poor prognosis in human neuroendocrine cancers, PNAS 102 (28) (2005) 9901–9906.
[21] J.C. Lindon, J.K. Nicholson, E. Holmes, H.C. Keun, A. Craig, J.T. Pearce, et al., Summary recommendations for standardization and reporting of metabolic analyses, Nat. Biotechnol. 23 (7) (2005) 833–839.
[22] J. Casado-Vela, A. Cebrián, M.T.G. del Pulgar, et al., Approaches for the study of cancer: towards the integration of genomics, proteomics and metabolomics, Clin. Transl. Oncol. 13 (9) (2011) 617–628.
[23] M. Villar, N. Ayllon, P. Alberdi, A. Moreno, M. Moreno, R. Tobes, L. Mateos-Hernandez, S. Weisheit, L. Bell-Sakyi, J. de la Fuente, Integrated Metabolomics, Transcriptomics and Proteomics Identifies Metabolic Pathways Affected by Anaplasma phagocytophilum Infection in Tick Cells, Mol. Cell. Proteomics 14 (12) (2015) 3154–3172.
[24] Z.X. Peng, Y. Wang, X. Gu, Y. Xue, Q. Wu, et al., Metabolic transformation of breast cancer in a MCF-7 xenograft mouse model and inhibitory effect of volatile oil from Saussurea lappa Decne treatment, Metabolomics 11 (3) (2015) 636–656.
[25] J. Kloppenborg, C.E. Fonvig, J. Johannesen, P.J. Bjerrum, H.E. Poulsen, J.C. Holm, Urinary markers of nucleic acid oxidation in Danish overweight/obese children and youths, Free Rad. Res. 50 (7) (2016) 691–697.
[26] B. Denard, C. Lee, J. Ye, Doxorubicin blocks proliferation of cancer cells through proteolytic activation of CREB3L1, eLife 1 (2012) e00090, https://doi.org/10.7554/elife.00090.
[27] F. Frezard, A. Garnier-Suillerot, Comparison of the membrane transport of anthracycline derivatives in drug-resistant and drug-sensitive K562 cells, Eur. J. Biochem. 196 (2) (1991) 483–491.
[28] C. Wen, L. Fu, J. Huang, Y. Dai, B. Wang, et al., Curcumin reverses doxorubicin resistance via inhibition the efflux function of ABCB4 in doxorubicin-resistant breast cancer cells, Mol. Med. Rep. 19 (6) (2019) 5162–5168.
[29] J.P. Xue, G. Wang, Z.B. Zhao, Q. Wang, Y. Shi, Synergistic cytotoxic effect of genistein and doxorubicin on drug-resistant human breast cancer MCF-7/Adr cells, Oncol. Rep. 32 (4) (2014) 1647–1653.
[30] A.L. Luss, P.P. Kulikov, S.B. Romme, C.L. Andersen, C.P. Pennisi, A.O. Docea, et al., Nanosized carriers based on amphiphilic poly-N-vinyl-2-pyrrolidone for intranuclear drug delivery, Nanomedicine (Lond.) 13 (7) (2018) 703–715.
[31] R.B. James, E. Balmer, Gene expression regulation by retinoic acid, J. Lipid Res. 43 (11) (2002) 1773–1808.
[32] Y.P. Du, J.S. Peng, A. Sun, Z.H. Tang, W.H. Ling, H.L. Zhu, Assessment of the effect of betaine on p16 and c-mycDNA methylation and mRNA expression in a chemical induced rat liver cancer model, BMC Cancer 9 (1) (2009) 1–9.
[33] B.-V. Nusgens, Hyaluronic acid and extracellular matrix: a primitive molecule? Annales de Dermatologie et de Vénéréologie 137 (2010) S3–8.
[34] H. Aoyama, Y. Kamiyama, M. Ukikusa, K. Ozawa, Clinical significance of hippurate-synthesizing capacity in surgical patients with liver disease: a metabolic tolerance test, J. Lab. Clin. Med. 108 (5) (1986) 448–455.